Elastic electron scattering by a Pb atom

S. D. Tošić,[1] M. S. Rabasović,[1] D. Šević,[1] V. Pejčev,[1,2] D. M. Filipović,[1,3] Lalita Sharma,[4] A. N. Tripathi,[4] Rajesh Srivastava,[4] and B. P. Marinković[1]

[1]*Institute of Physics, Pregrevica 118, 11080 Belgrade, Serbia*

[2]*Faculty of Natural Sciences, Radoja Domanovića 12, 34000 Kragujevac, Serbia*

[3]*Faculty of Physics, University of Belgrade, P.O. Box 368, 11001 Belgrade, Serbia*

[4]*Department of Physics, Indian Institute of Technology, Roorkee 247667, India*

(Received 8 November 2007; published 31 January 2008)

Differential (DCS), integral (Q_I), momentum transfer (Q_M), and viscosity (Q_V) cross sections are obtained both experimentally and theoretically for elastic electron scattering by lead atoms in the energy range from 10 to 100 eV. The experiment is performed using an electron spectrometer with crossed electron and atom-beam arrangement. The relative DCS measurements are placed on an absolute scale using measured elastic-to-inelastic intensity ratios and the absolute DCS of the $6p7s\ ^3P_1$ state [S. Milisavljević, M. S. Rabasović, D. Šević, V. Pejčev, D. M. Filipović, L. Sharma, R. Srivastava, A. D. Stauffer, and B. P. Marinković, Phys. Rev. A **76**, 022714 (2007)] at a scattering angle of 10° for incident energies of 40, 60, 80, and 100 eV and at 30° for 10 and 20 eV. Corresponding theoretical results are obtained from a relativistic approach based on solving the Dirac equation using Hartree-Fock and Dirac-Fock wave functions to calculate cross sections at all the energies measured. Comparisons between the present experiment and theory, as well as comparisons with other available results, have been made.

DOI: 10.1103/PhysRevA.77.012725 PACS number(s): 34.80.Bm

I. INTRODUCTION

In our previous papers [1,2] we reported results for both experimental and theoretical investigations of inelastic electron collision with Pb atoms. Here we focus our attention on elastic electron scattering by the same target. It is well known that electron-atom collisions can be described by many theoretical approaches and that is why it is important to test the various approximations with experimental measurements. At the same time, elastic scattering is of critical importance in many fields, including the physics of stars and plasmas [3]. Collaboration between experimental and theoretical research groups makes detailed investigations of the collision dynamics possible. Experimental and theoretical studies of the electron scattering by Pb atoms, performed so far, are very limited. This is especially the case in the research area which focuses on determining differential cross sections (DCSs) in the energy range considered in this paper.

The experimental work on angular dependences of DCSs is limited to only one result at 40 eV by Williams and Trajmar [4]. They measured both elastic and several inelastic features at this single energy and scattering angles up to 140°. Bartschat [5] applied the relativistic *R*-matrix calculation to the low energy (0–7 eV) electron scattering. He presented results for the Sherman function, total elastic cross sections at energies up to 6 eV, DCS at an incident electron energy of 1.9 eV, and also analyzed the positions and role of the resonances. In the polarization experiment by Kaussen *et al.* [6] unpolarized electrons were scattered elastically from unpolarized Hg, Tl, Pb, and Bi atoms and the polarization of the scattered electrons was measured for scattering angles between 30° and 130° in the energy range from 6 to 180 eV. Haberland and Fritsche [7] also investigated spin polarization in elastic scattering of low-energy electrons by the same atoms using a generalized Kohn-Sham one-particle theory. Geesmann *et al.* [8] measured the left-right asymmetry of polarized electrons scattered from unpolarized Tl and Pb atoms at energies below 6 eV. Using the Dirac *R*-matrix method, Wijesundera *et al.* [9] calculated total cross sections for elastic scattering in the region from 0 to 4 eV and also identified and analyzed resonances in the same energy range. Kumar *et al.* [10] calculated spin-polarization parameters, differential, integral, momentum transfer, and total cross sections for the elastic scattering of electrons by zinc and lead atoms at energies up to 200 eV using both real (RP) and complex (CP) potentials within the framework of the relativistic Dirac equation. Werner [11] reported DCSs at energies from 100 to 10 000 eV. He utilized the numeric code of Yates [12] and solved the Dirac equations using an empirical potential from the paper of Bonham and Strand [13] as input. In this approach the polarization and the exchange potentials are not taken into account and, as we will discuss here, this affects the angular dependence of the calculated DCS in the forward direction. Fink and Yates [14] used relativistic Hartree-Fock-Slater scattering potentials to solve the Dirac equations. This calculation also excluded the exchange of the incoming electron with the atomic electrons, which leads to results very similar to those by Werner [11].

We present here the results of both experimental and theoretical studies of elastic electron scattering by Pb atoms. We measured the angular distribution of elastically scattered electrons in the intermediate energy range up to 100 eV at scattering angles from 10° to 150°. At scattering angles less than 10° measurements are not performed due to the possible influence of the primary electron beam. Theoretical analysis using Hartree-Fock (HF) and Dirac-Fock (DF) wave functions are also carried out. The results for DCSs, integral (Q_I), momentum transfer (Q_M), and viscosity (Q_V) cross sections are compared with the other experimental measurement [4] as well as previous calculations [7,10,11,14].

II. EXPERIMENTAL TECHNIQUES AND PROCEDURES

The crossed electron-atom beam apparatus was used in [1,2] to measure DCS for inelastic electron-Pb scattering. Thus we will only give a brief outline of the experimental setup and measurement procedure and conditions which was described in detail in our earlier publications. The apparatus consists of a crossed beam hemispherical electron spectrometer with a channel electron multiplier as a single electron detector and a hairpin thermoelectron source. Both the monochromator and analyzer are of the same type (systems of cylindrical electrostatic lenses made of gold-plated oxygen-free high conductivity (OFHC) copper and spheres made of molybdenum). All of these components are enclosed in a double μ-metal shielded vacuum chamber with the background pressure of the order of 10^{-5} Pa. An atomic oven heated by two resistive bifilar heaters is used to produce a well-collimated effusive Pb vapor beam. The stability of the target beam is checked and controlled by monitoring the temperature at the bottom (below 1200 K) and at the top of the crucible.

The elastically scattered electron intensities at E_0=10, 20, 40, 60, 80, and 100 eV are detected as a function of scattering angle ranging from 10° to 150° and then converted to relative DCSs using the effective path length correction factors [15] determined for the current experimental conditions. The absolute DCS values at 40, 60, 80, and 100 eV incident electron energies are obtained from measured elastic to inelastic intensity ratios and using the absolute DCS of the $6p7s\ ^3P_1$ state of Pb at 10° [1,2]. In order to avoid the possible influence of the primary electron beam, absolute DCSs at 10 and 20 eV are determined using the ratios of the elastic scattering intensity to the inelastic intensity from energy-loss spectra recorded at a scattering angle of 30°. At these impact energies it was also necessary to include the corrections due to the variation of analyzer transmission in the energy-loss spectra. Absolute elastic DCSs are extrapolated to 0° and 180° and numerically integrated to obtain integral, momentum transfer, and viscosity cross sections [Eqs. (1)–(3) in [2]]. Integral cross sections strongly depend on the DCS extrapolation to 0° scattering angle while the extrapolation to 180° scattering angle affects the momentum transfer cross sections significantly. In order to extend experimental DCSs to 0° and 180° scattering angles and since the major contribution to Q_I comes from strongly forward peaked DCSs at small scattering angles, the extrapolation is performed in three different ways. First, we used the shapes of the DF calculations, second, we used results calculated in the HF approximation (normalized to experimentally obtained DCSs at 10° and 150°), third, we applied polynomial fits to extrapolate our DCS values. The contributions of different extrapolation techniques are also analyzed.

III. CALCULATION METHOD

In this calculation the motion of the projectile electron in a central field $V(r)$ is described by the Dirac equation

$$[c\boldsymbol{\alpha}\cdot\mathbf{p}+\beta mc^2-V(r)]\psi=E\psi, \tag{1}$$

where $E=mc^2=m_0\gamma c^2=E_i+m_0c^2$ is the total energy, $\gamma=(1-v^2/c^2)^{-1/2}$, and E_i is the kinetic energy of the incident particle having rest mass m_0 and velocity v. $\boldsymbol{\alpha}$ and β are the usual 4×4 Dirac matrices. The spinor ψ has four components, $\psi=(\psi_1,\psi_2,\psi_3,\psi_4)$, where (ψ_1,ψ_2) are the large components and (ψ_3,ψ_4) are the small components of ψ. For a central potential the Dirac equation can be reduced to a set of two equations similar to the form of Schrödinger equation [10,16]

$$g_\ell^{\pm\prime\prime}+\left(k^2-\frac{\ell(\ell+1)}{r^2}-U_\ell^\pm(r)\right)g_\ell^\pm(r)=0, \tag{2}$$

where $g_\ell^\pm$ is related to the radial part $G_\ell^\pm$ of the large component of ψ by $G_\ell^\pm=\sqrt{\eta}g_\ell/r$, $\eta=(E-V+m_0c^2)/\hbar c$, and $k^2=(E^2-m_0^2c^4)/\hbar^2c^2$. The effective Dirac potential terms $U_\ell^\pm(r)$ expressed in atomic units are given by

$$-U_\ell^\pm(r)=-2\gamma V+\alpha^2V^2-\frac{3}{4}\frac{\eta'^2}{\eta^2}+\frac{1}{2}\frac{\eta''}{\eta}\pm\left(\frac{\ell+1}{\ell}\right)\frac{1}{r}\frac{\eta'}{\eta}, \tag{3}$$

where α is the fine-structure constant (not to be confused with the Dirac matrix $\boldsymbol{\alpha}$). The single and double primes correspond to the first and second derivatives with respect to r, respectively. It should be noted that the last term of $U_\ell^\pm(r)$ in Eq. (3) corresponds to two eigenvalues of the well-known spin-orbit interaction,

$$\frac{1}{4m_0^2c^2}\frac{1}{r}\frac{dV(r)}{dr}\boldsymbol{\sigma}\cdot\mathbf{L}, \tag{4}$$

one due to spin up and the other due to spin down. Here, $\boldsymbol{\sigma}$ is related to the spin $\mathbf{S}$ as $\boldsymbol{\sigma}=2\mathbf{S}$ and the value of $\langle\boldsymbol{\sigma}\cdot\mathbf{L}\rangle$ equals ℓ for $j=(\ell+1/2)$ and $-(\ell+1)$ for $j=(\ell-1/2)$.

The proper solution of Eq. (2) behaves asymptotically as

$$g_\ell^\pm(k,r)\sim kr[j_\ell(kr)-\tan\delta_\ell^\pm\eta_\ell(kr)],\quad \text{for } r\to\infty, \tag{5}$$

where j_ℓ and η_ℓ are the spherical Bessel functions of the first and second kind, respectively, and $\delta_\ell^\pm$ are the scattering phase shifts. The plus sign corresponds to the incident particle with spin up and the minus sign to spin down. These phase shifts $\delta_\ell^\pm$ are obtained from the asymptotic values of the radial wave function by numerical integrating Eq. (2) using the Numerov method.

The two complex scattering amplitudes $f(k,\theta)$ (the direct amplitude) and $g(k,\theta)$ (the spin flip amplitude) are defined as (see Ref. [17])

$$f(k,\theta)=\frac{1}{2ik}\sum_{\ell=0}^{\infty}((\ell+1)[e^{2i\delta^+}-1]+\ell[e^{2i\delta^-}-1])P_\ell(\cos\theta), \tag{6}$$

$$g(k,\theta)=\frac{1}{2ik}\sum_{\ell=1}^{\infty}(e^{2i\delta^-}-e^{2i\delta^+})P_\ell^1(\cos\theta), \tag{7}$$

where θ is the scattering angle and $P_\ell(\cos\theta)$ and $P_\ell^1(\cos\theta)$ are Legendre polynomials and Legendre associated functions, respectively. The elastic differential cross section for scattering of the unpolarized incident electron beam is given by

TABLE I. The parameters for the description of polarization potential.

Atomic number	Electronic configuration	Term	Polarizability (a.u.)	IP (eV)	E_{th} (eV)	Crossing point (a.u.)
82	$[Xe]6s^24f^{14}5d^{10}6p^2$	^3P	45.89	7.42	4.64	14.0

$$\sigma(\theta) = \frac{d\sigma}{d\Omega} = |f|^2 + |g|^2. \quad (8)$$

Here, the total interaction between an electron and a target atom is approximated by an effective potential $V(r)$. The real part of this potential is chosen to be sum of three terms, the static (V_{st}), exchange (V_{ex}), and polarization (V_{pol}) potentials. These potential terms are functions of the electronic density of the target and approximately account for the dynamics of the collision. The static potential $V_{st}(r)$ and the charge density $\rho(r)$ are obtained using the nonrelativistic Slater-type orbitals of Roothann in Hartree-Fock wave functions as given by Mclean and Mclean [18]. In addition, we have also used relativistic Dirac-Fock wave function obtained from the GRASP92 code of Parpia *et al.* [19] to compute $V_{st}(r)$ and $\rho(r)$.

In the present calculations, we use a modified semiclassical exchange (MSCE) potential as given by Gianturco and Scialla [20] for the exchange potential (V_{ex}). For the polarization potential (V_{pol}), we use a parameter-free polarization potential based on the correlation energy of the target atom. It has two components, the short-range $V_{SR}(r)$ and the long-range $V_{LR}(r)$ parts and is given by

$$V_{pol} = \begin{cases} V_{\mathrm{SR}}(r), & r < r_c \\ V_{LR}(r), & r \geqslant r_c. \end{cases}$$

Here r_c is the point where the two forms cross each other for the first time. The short-range form for electron scattering from atoms is based on the free electron gas exchange potential and is given by

$$V_{SR}(r) = \begin{cases} 0.0622 \ln r_s - 0.096 + 0.018 r_s \ln r_s - 0.02 r_s, & r_s \leqslant 0.7, \\ -0.1231 + 0.03796 \ln r_s, & 0.7 < r_s \leqslant 10, \\ -0.876 r_s^{-1} + 2.65 r_3^{-3/2} - 2.8 r_s^{-2} - 0.8 r_s^{-5/2}, & 10 \leqslant r_s, \end{cases}$$

where $r_s = (3/4\pi\rho(r))^{1/3}$ and $\rho(r)$ is the electronic charge density of the target system. The long-range form of the polarization potential is given by $V_{LR} = -\alpha_d / 2r^4$ where α_d is the static dipole polarizability. The crossing point for the lead atom along with its dipole polarizability, ionization potential (IP), and first excitation threshold are listed in Table I. Finally, in order to account for all the inelastic processes during the scattering, we also add the modified version of the semirelativistic model absorption potential of Staszewska *et al.* [21] as given in the paper of Neerja *et al.* [22].

IV. RESULTS AND DISCUSSION

Experimental elastic DCSs are obtained in the energy range from 10 to 100 eV at scattering angles from 10° to 150° while the calculations are performed using both the Hartree-Fock (HF) and the Dirac-Fock (DF) wave functions. All experimentally obtained cross sections for elastic electron scattering by lead atoms are given in Table II and presented graphically in Figs. 1–3. They are compared with the current calculations, and other available results. The extrapolated experimental values using the normalized shape of the calculated DCSs using DF wave functions are also given in Table II. Figure 1 shows differential cross sections at 10, 20, and 40 eV incident electron energies. For 10 eV [Fig. 1(a)], we observe good agreement in shape and magnitude between the present experimental and DF results at angles $<110°$ while at higher angles experiment gives significantly smaller DCSs. In contrast, the HF calculation produces larger cross sections over the entire range of scattering angles. We also observe that both the HF and DF calculations and experiment give one broad minimum between 90° and 100°. The results of Haberland and Fritsche [7] at 11 eV are also shown in Fig. 1(a). They are derived from scattering amplitudes for direct and spin-flip scattering as presented by Kaussen *et al.* [6]. There is a good agreement in absolute values between the results of Haberland and Fritsche [7] and our results, despite the 1 eV difference in energy. For 20 eV [Fig. 1(b)] the experimental data are in better agreement with those obtained from the HF calculations while the DF calculations show slight discrepancies in shape as compared with our measurements and HF results. They differ from the other present data especially in the positions of the first and the second minima. At 40 eV incident electron energy [Fig. 1(c)], three minima at 40°, 90°, and 140° are observed in our experiment. Both the HF and DF calculations also predict three minima with the second minimum slightly shifted towards smaller scattering angles as compared to the experimental data. The only available previous experimental data of Williams and Trajmar [4] are also included for comparison. The DCSs agree well in shape, but the present data are lower over the entire

TABLE II. Differential cross sections, in units of 10^{-20} m^2 sr^{-1}, for elastic electron scattering by Pb. The numbers in parentheses are absolute errors. The extrapolated values are given in square brackets. The last three lines are integral (Q_I), momentum transfer (Q_M), and viscosity (Q_V) cross sections obtained by integrating our measured DCS in units of 10^{-20} m^2 with absolute errors indicated in parentheses.

Angle (deg)	Electron energy					
	10 eV	20 eV	40 eV	60 eV	80 eV	100 eV
0	[56.718]	[130.408]	[162.296]	[133.672]	[118.215]	[143.591]
10	33.0(7.9)	54(10)	38.1(6.8)	20.3(3.8)	14.1(2.8)	15.4(2.8)
20	14.1(3.4)	16.6(3.2)	6.9(1.2)	3.30(61)	2.78(55)	3.16(57)
30	5.3(1.3)	3.50(66)	1.11(20)	1.28(24)	1.20(24)	1.12(20)
40	1.54(37)	0.337(64)	0.58(11)	0.79(15)	0.61(12)	0.423(76)
50	0.54(13)	0.218(42)	0.91(16)	0.432(80)	0.263(52)	0.141(25)
60	0.210(50)	0.458(87)	0.98(18)	0.245(46)	0.113(22)	0.069(12)
70	0.115(28)	0.412(79)	0.69(12)	0.138(26)	0.094(19)	0.071(13)
80	0.056(14)	0.174(33)	0.189(36)	0.114(22)	0.117(23)	0.082(15)
90	0.0266(66)	0.0409(82)	0.073(15)	0.141(27)	0.136(27)	0.080(14)
100	0.0289(72)	0.091(18)	0.342(63)	0.212(40)	0.133(26)	0.058(10)
110	0.048(12)	0.224(43)	0.83(15)	0.286(53)	0.105(21)	0.0293(53)
120	0.076(18)	0.219(42)	0.95(17)	0.291(54)	0.082(16)	0.0123(22)
130	0.105(25)	0.077(15)	0.67(12)	0.177(33)	0.0432(86)	0.0062(11)
140	0.149(36)	0.157(30)	0.168(32)	0.0454(89)	0.0175(36)	0.0080(15)
150	0.238(57)	0.74(14)	0.293(54)	0.055(11)	0.0412(82)	0.0175(32)
160	[0.323]	[1.388]	[1.005]	[0.306]	[0.122]	[0.033]
170	[0.390]	[1.966]	[1.861]	[0.605]	[0.205]	[0.049]
180	[0.415]	[2.196]	[2.241]	[0.736]	[0.240]	[0.055]
Q_I	18.0(7.1)	24.8(6.7)	21.0(6.3)	11.6(3.5)	8.4(2.6)	8.3(2.3)
Q_M	3.4(1.4)	5.7(1.5)	7.8(2.6)	2.9(1.0)	1.5(0.5)	0.8(0.3)
Q_V	4.3(1.9)	4.4(1.5)	5.1(1.8)	2.3(0.8)	1.4(0.6)	1.0(0.3)

range of scattering angles. There are two possible explanations for this disagreement. In our previous study focused on electron impact excitation of the $6p7s\ ^3P_{0,1}$ states of Pb atoms [2] we compared our measured cross sections with the corresponding results of the same authors [4]. In this case, we also found significant disagreement in absolute values, with our results being lower by approximately a factor of 15 to 20. We concluded then that these differences were probably due to the normalization procedure applied. On the other hand, since Williams and Trajmar have also used ratios of the elastic to inelastic intensities from energy-loss spectra at different scattering angles to obtain absolute elastic cross sections, we compared their ratios with ours. In our experiment we obtained ratios approximately 2.5 to 3 times larger. Although these two factors partially cancel, we found that our elastic cross sections are smaller by a factor of 5 to 8.

The agreement between the measured DCSs and those calculated using HF and DF wave functions at 60 eV shown in Fig. 2(a) is quite good especially at lower scattering angles (less than 70°). On the other hand, both calculations show a significantly deeper minimum around 140° where measurements produce one shallow minimum. A similar trend is found at 80 eV incident electron energy [Fig. 2(b)]. The present experimental results are in good agreement with theory except for the minimum near 140°, where the disagreement in absolute value is quite significant. It is also evident that, at energies higher than 60 eV, there are decreasing differences between the calculated HF and DF results. Finally, in Fig. 2(c) we present results for the differential cross sections at 100 eV. The DCSs calculated using HF and DF wave functions agree well in shape with the measured data (see inset) but lie above the experiment in magnitude over the whole angular range except near 130°. However, in this range the DF calculations predict a more pronounced minimum. This is also true for the data by Kumar *et al.* [10]. Their RP and CP results are almost identical to the DF calculations up to 130°. At higher scattering angles, however, they are somewhat smaller compared to the cross sections calculated here.

The agreement between experiment and calculation by Werner [11] is quite good except at angles below 50° where Werner's data are less forward peaked. This behavior is attributed to the fact that polarization and exchange effects are not included in the calculations. Exchange is also not taken into account in the old calculation by Fink and Yates [14] which produces very similar results except for a lower minimum around 130°. Since both polarization and exchange potentials are necessary ingredients in the present state of sophisticated elastic scattering calculations, one can conclude that good agreement with both Werner and Fink and Yates's

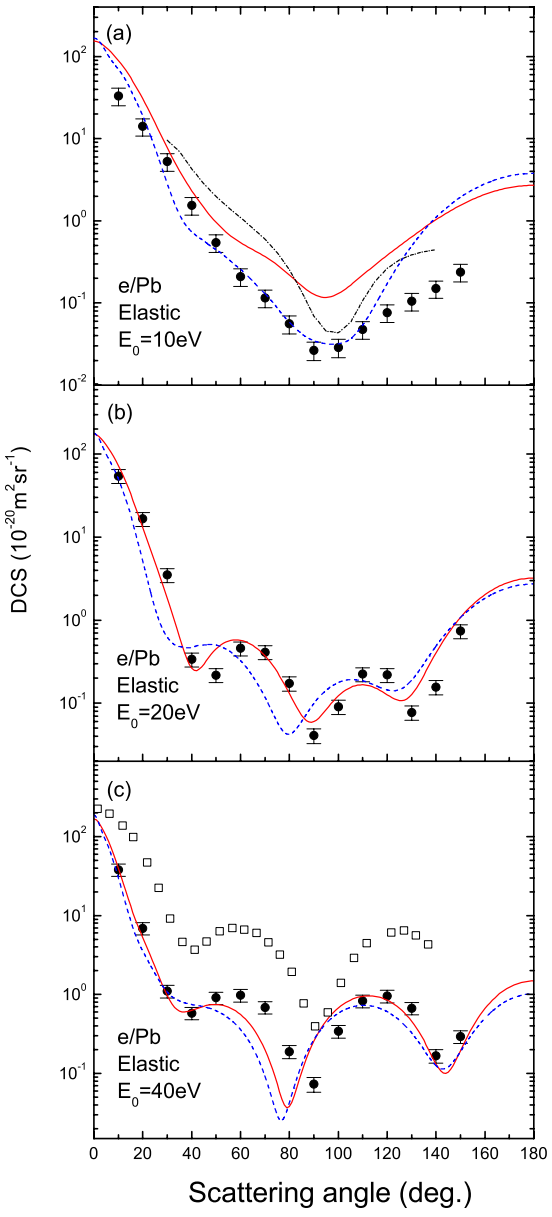

FIG. 1. (Color online) Differential cross sections for the elastic electron scattering by lead atoms at (a) 10 eV, (b) 20 eV, and (c) 40 eV electron-impact energies. Filled circles with error bars denote the present experimental results. The solid line shows DCSs calculated using the HF wave function and the dashed line shows the results obtained using the DF wave function. The short dashed-dotted line denotes calculated DCS values from the results of Haberland and Fritsche [7] at 11 eV derived from scattering amplitudes for direct and spin-flip scattering as presented by Kaussen *et al.* [6]. The open squares represent the results obtained by Williams and Trajmar [4].

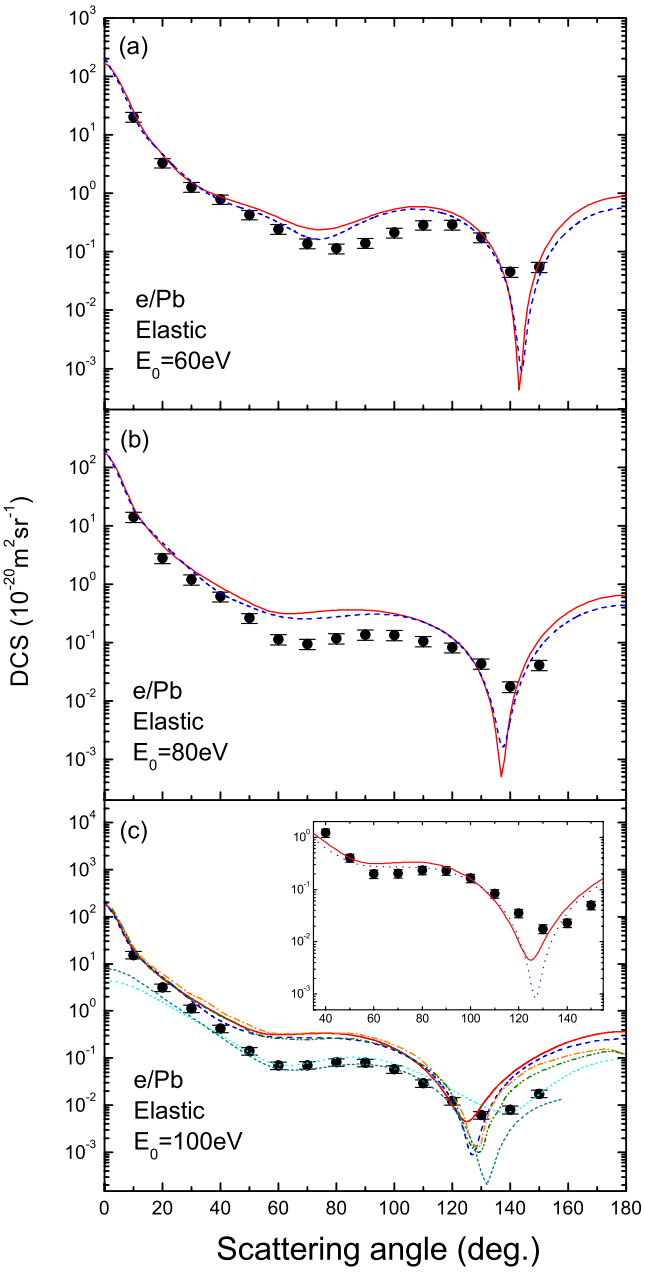

FIG. 2. (Color online) As for Fig. 1 except for (a) 60 eV, (b) 80 eV, and (c) 100 eV electron-impact energies. The dashed-dotted-dotted and dashed-dotted lines show the CP and RP results by Kumar *et al.* [10]. The dotted lines denote the calculations by Werner [11]. In the inset, the present experimental DCSs are normalized at 50° to the present DF calculations. The short dashed line denotes results by Fink and Yates [14].

calculated differential cross sections is fortuitous.

As mentioned in Sec. II, we extrapolated our experimental DCSs to 0° and 180° using the DF and HF calculated DCS profiles. We believe that this is valid considering the reasonably good agreement in shape between the experiment and theory (and the fact that the DF and HF results approach each other as the impact energies increase). We also performed a polynomial extrapolation. All extrapolations give very similar results for integrated cross sections with the comparable contributions of the extrapolated values agreeing within few percent. The largest contributions of the extrapolated region to Q_I, up to 50%, are obtained at higher impact energies. The extrapolated values also give large contributions to Q_M (up to 45% at 20 eV), while for Q_V, the contributions are smaller than 7% at all impact energies. Our present results using the shape of our DCSs calculated in the

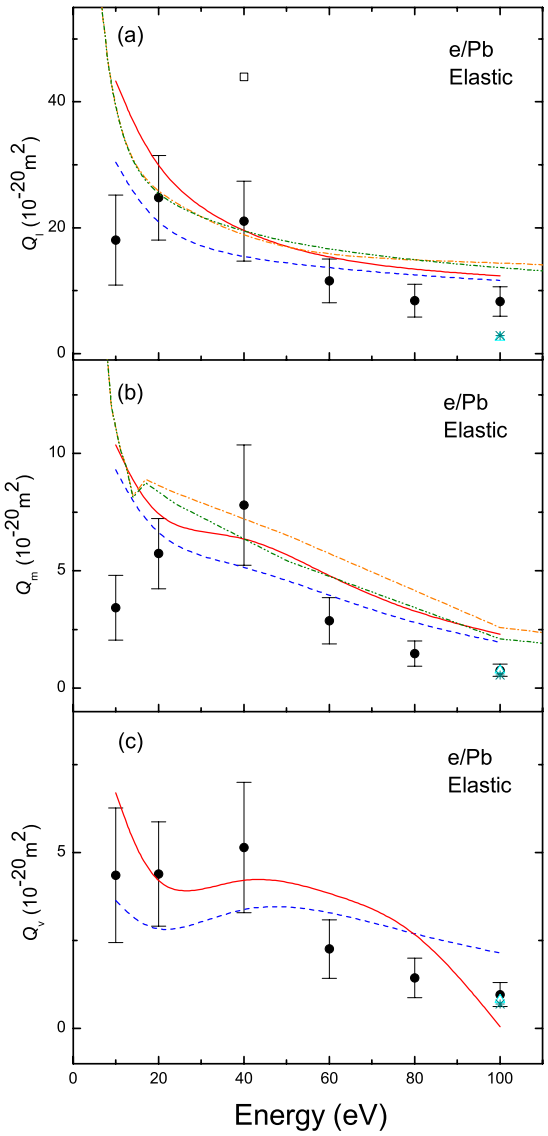

FIG. 3. (Color online) (a) Integral, (b) momentum transfer, and (c) viscosity cross sections for elastic electron scattering by lead atoms. Experiment and theories are as for Fig. 2. Open triangles denote results by Werner [11] while stars represent results obtained by Fink and Yates [14].

Dirac-Fock approximation for extrapolation are shown in Fig. 3 for the integral (Q_I), momentum transfer (Q_M), and viscosity (Q_V) cross sections for elastic scattering of electrons by lead atoms and compared with the other available results. The present experiment shows good agreement with the present HF and DF calculations and also with the RP and CP calculations [10] for $E_0 \geqslant 20$ eV [Fig. 3(a)], while at the lowest energy of 10 eV the experiment gives a somewhat smaller Q_I value. The good agreement between the experimental and DF results for Q_I is consistent with the agreement in the shape of the DCSs and the fact that the extrapolations are based on the shape of the calculated DF DCSs values. The experimental result by Williams and Trajmar [4] at 40 eV is much higher than all other values, which is not unexpected considering that their DCS results are higher than ours over the entire range of scattering angles. The present experimental Q_M values rise in the energy range from 10 eV to 40 eV and thereafter decrease with increasing incident electron energy [Fig. 3(b)]. The RP and CP results [10] also show similar features with a minimum at 14 eV. All calculated Q_M values except those of Werner and Fink and Yates are higher than the experimental data at 60, 80, and 100 eV. The experiment confirms a decrease of Q_V with increasing incident electron energy from 40 eV to 100 eV [Fig. 3(c)] and shows good agreement with the DF and HF calculations. The present measured data for incident electron energies of 10 and 20 eV also agree well with both the HF and DF calculations.

V. CONCLUSIONS

We investigated elastic electron scattering from Pb atoms by measuring and calculating differential and integrated cross sections at energies up to 100 eV. These results supplement our earlier investigations of inelastic scattering processes in the electron-lead system. The experiment is based on a crossed beam technique while calculations are carried out using both Hartree-Fock and Dirac-Fock wave functions in a relativistic optical potential method. In general, we found good agreement between the measured data and the theoretical calculations. We also noted the energies and scattering angles where the match between experiment and theory needs to be improved. We believe that this work might lead to additional theoretical investigations resulting in better agreement with the measured results at all energies and more accurate modeling of the elastic electron interaction with Pb atoms.

ACKNOWLEDGMENTS

This work has been carried out within Project No. 141011 financed by Ministry of Science of Republic of Serbia. One of us (A.N.T.) gratefully acknowledges additional support from University Grant Commission (UGC) New Delhi. We thank Professor Al Stauffer and Dr. Darko Popović for a critical reading of the manuscript.

[1] S. Milisavljević, M. S. Rabasović, D. Šević, V. Pejčev, D. M. Filipović, L. Sharma, R. Srivastava, A. D. Stauffer, and B. P. Marinković, Phys. Rev. A **75**, 052713 (2007).
[2] S. Milisavljević, M. S. Rabasović, D. Šević, V. Pejčev, D. M. Filipović, L. Sharma, R. Srivastava, A. D. Stauffer, and B. P. Marinković, Phys. Rev. A **76**, 022714 (2007).
[3] C. J. Horowitz, Eur. Phys. J. A **24**, 167 (2005).
[4] W. Williams and S. Trajmar, J. Phys. B **8**, L50 (1975).

[5] K. Bartschat, J. Phys. B **18**, 2519 (1985).
[6] F. Kaussen, H. Geesmann, G. F. Hanne, and J. Kessler, J. Phys. B **20**, 151 (1987).
[7] R. Haberland and L. Fritsche, J. Phys. B **20**, 121 (1987).
[8] H. Geesmann, M. Bartsch, G. F. Hanne, and J. Kessler, J. Phys. B **24**, 2817 (1991).
[9] W. P. Wijesundera, I. P. Grant, and P. H. Norrington, J. Phys. B **25**, 2165 (1992).
[10] P. Kumar, A. K. Jain, A. N. Tripathi, and S. N. Nahar, Phys. Rev. A **49**, 899 (1994).
[11] Available at http://www.iap.tuwien.ac.at/~werner/data_ecs.html
[12] A. C. Yates, Comput. Phys. Commun. **2**, 175 (1971).
[13] A. Bonham and T. G. Strand, J. Chem. Phys. **39**, 2200 (1963).
[14] M. Fink and A. C. Yates, At. Data **1**, 385 (1970).
[15] R. T. Brinkmann and S. Trajmar, J. Phys. E **14**, 245 (1981).
[16] S. N. Nahar and J. M. Wadehra, Phys. Rev. A **43**, 1275 (1991).
[17] C. J. Joachain, *Quantum Collision Theory* (North Holland, Amsterdam, 1983).
[18] A. D. Mclean and R. S. Mclean, At. Data Nucl. Data Tables **26**, 197 (1981).
[19] F. A. Parpia, C. Froese Fischer, and I. P. Grant, Comput. Phys. Commun. **94**, 249 (1996).
[20] F. A. Gianturco and S. Scialla, J. Phys. B **20**, 3171 (1987).
[21] G. Staszewska, D. W. Schwenke, and D. G. Truhlar, Phys. Rev. A **29**, 3078 (1984).
[22] Neerja, A. N. Tripathi, and A. K. Jain, Phys. Rev. A **61**, 032713 (2000).